Environmental Research Letters

LETTER • **OPEN ACCESS**

Winter Eurasian cooling linked with the Atlantic Multidecadal Oscillation

To cite this article: Dehai Luo *et al* 2017 *Environ. Res. Lett.* **12** 125002

View the article online for updates and enhancements.

This content was downloaded from IP address 223.104.255.72 on 22/11/2017 at 17:57

Environmental Research Letters

LETTER

Winter Eurasian cooling linked with the Atlantic Multidecadal Oscillation

Dehai Luo[1,2,3,4,8], **Yanan Chen**[1,2], **Aiguo Dai**[5], **Mu Mu**[6], **Renhe Zhang**[6] **and Ian Simmonds**[7]

1 CAS Key Laboratory of Regional Climate-Environment for Temperate East Asia, Institute of Atmospheric Physics, Chinese Academy of Sciences, Beijing, 100029, People's Republic of China
2 University of Chinese Academy of Sciences, Beijing, People's Republic of China
3 Physical Oceanography Laboratory/CIMST, Ocean University of China, Qingdao, People's Republic of China
4 Qingdao National Laboratory for Marine Science and Technology, Qingdao, People's Republic of China
5 Department of Atmospheric and Environmental Sciences, State University of New York at Albany, SUNY, Albany, NY 12222, United States of America
6 Institute of Atmospheric Science, Fudan University, Shanghai, People's Republic of China
7 School of Earth Sciences, The University of Melbourne, Victoria, Australia
8 Author to whom any correspondence should be addressed.

E-mail: ldh@mail.iap.ac.cn

Keywords: Atlantic Multidecadal Oscillation, Eurasian cooling, Arctic sea ice decline, Shape and persistence of Ural blocking

Supplementary material for this article is available online

OPEN ACCESS

RECEIVED
27 June 2017

REVISED
14 September 2017

ACCEPTED FOR PUBLICATION
20 September 2017

PUBLISHED
22 November 2017

Original content from this work may be used under the terms of the Creative Commons Attribution 3.0 licence.

Any further distribution of this work must maintain attribution to the author(s) and the title of the work, journal citation and DOI.

Abstract

In this paper, we analyze observational and reanalysis data to demonstrate that the Atlantic Multidecadal Oscillation (AMO) significantly modulates winter Eurasian surface air temperature through its impact on the shape, frequency and persistence of Ural blocking (UB) events that last for 10–20 d. This impact results from changes in mid-high latitude westerly winds over Eurasia associated with the warming in the Barents–Kara Seas (BKS) through the AMO-driven high sea surface temperature and sea-ice decline and resultant weakening in meridional temperature gradients. The BKS warming has a strongest positive correlation with the AMO at a time lag of about 14 years. During the recent positive AMO phase, more persistent northwest–southeast (NW–SE) oriented UB events are favored by weakened westerly winds in Eurasian mid-high latitudes. Through cold atmospheric advection and radiative cooling, such UB events produce a strong, persistent and widespread cooling over Eurasia and enhance BKS warming during 1999–2015. However, the positive AMO phase cannot directly produce the Eurasian cooling if the UB is absent. Thus, we conclude that the recent AMO phase change is a major cause of the recent winter cooling over Eurasia through its impact on BKS temperature and sea ice, which in turn affect the meridional temperature gradient, the westerly winds and the UB events.

1. Introduction

Rapid winter warming over the Arctic and large winter cooling over Eurasia are the most important manifestations of the recent climate change over northern latitudes (Cohen *et al* 2014). While some studies have attributed the Arctic warming to anthropogenic forcing (Gillett *et al* 2008), Arctic surface air temperature (SAT) and sea-ice cover (SIC) were found to exhibit clear multidecadal variations associated with the Atlantic Multidecadal Oscillation (AMO) (Levitus *et al* 2009, Wyatt *et al* 2012, Mahajan *et al* 2011, Miles *et al* 2014), which reflects 60–80 year quasi-periodic oscillations in the sea surface temperature (SST) over the North Atlantic basin (Mann *et al* 1995, Knight *et al* 2005).

Many studies have indicated that the winter Eurasian temperature shows a clear multi-decadal variability linked to the AMO (Knight *et al* 2005, Wyatt *et al* 2012, Hao *et al* 2016), while it is also influenced by the North Atlantic Oscillation (NAO) (Li *et al* 2013, Hanna *et al* 2015), tropical forcing (Trenberth *et al* 2014), stratospheric processes (Scaife *et al* 2005, Omrani *et al* 2014), the Inter-decadal Pacific Oscillation (IPO) (Dai *et al* 2015, Steinman *et al* 2015) and decadal modulated oscillation (Huang *et al* 2017).

© 2017 The Author(s). Published by IOP Publishing Ltd

In particular, the winter Eurasian continent has exhibited a large cooling since the 1990s (Cohen *et al* 2014) that concurs with the recent global warming hiatus (Dai *et al* 2015, Huang *et al* 2017). Some studies have attributed the recent Eurasian cooling to recent winter sea-ice loss (Honda *et al* 2009, Outten and Esau 2012, Cohen *et al* 2014, Mori *et al* 2014, Kug *et al* 2015) because it is coincident with the Arctic sea-ice loss in the recent decades. However, a recent modeling study suggests that the winter Eurasian cooling is not related to the winter sea-ice loss in the Barents–Kara Seas (BKS), but may be due to other internally-generated atmospheric circulation anomaly patterns (McCusker *et al* 2016), while the atmospheric responses to the winter (Luo *et al* 2016a) and autumn (Wang *et al* 2017) sea ice anomalies are different. On the other hand, our recent studies (Luo *et al* 2016a Luo *et al* 2016b) suggest that individual Eurasian cold events are often linked to the presence of Ural blocking (UB) and their increased frequency can form a warm Arctic-cold Eurasia pattern to lead to a pause of global warming during 2000–2013 (Yao *et al* 2017, Deser *et al* 2017). The exact physical cause of the winter Eurasian cooling trend is still under debate (Semenov and Latif 2015, Kug *et al* 2015, Overland *et al* 2016, Huang *et al* 2017). In particular, it is unclear how the AMO contributes to the recent winter Eurasian cooling.

Because the SST and surface air temperature (SAT) over the BKS and sea-ice loss in winter are related to the AMO through the incursion of warm Atlantic water (Levitus *et al* 2009, Day *et al* 2012, Miles *et al* 2014), it is suggested that the AMO may affect the winter Eurasian cooling through its influence on the BKS warming related to the SIC decline in that the cold Eurasian anomaly occurs together with the BKS warming (Outten and Esau 2012, Cohen *et al* 2014, Luo *et al* 2016a). In this paper, we will investigate how the AMO influences the winter Eurasian temperature by analyzing observational and reanalysis datasets. We found that the AMO can contribute to the winter Eurasian cooling through changes in the frequency, persistence and shape of the UB patterns due to changes in westerly winds over Eurasia that are related to the BKS warming.

2. Data and method

The winter (December to February, DJF) daily data with $2.5° \times 2.5°$, which includes daily 500 hPa geopotential height, 500 hPa zonal wind and air temperature at 995 hPa defined as the SAT, is taken from the National Centers for Environmental Prediction-National Center for Atmospheric Research (NCEP-NCAR) reanalysis from December 1950 to February 2016 (1950–2015) (www.esrl.noaa.gov/psd/data/gridded/data.ncep.reanalysis.html). The data has been detrended for a linear trend during 1950–2015 and non-seasonalized.

The monthly mean SST and SIC data with $1° \times 1°$ grid points from 1950–2015 is available from the Hadley Centre Global Sea Ice and Sea Surface Temperature (HadISST) datase (www.metoffice.gov.uk/hadobs/hadisst/data/download.html). The winter AMO index during 1950–2015 is calculated by averaging the monthly SST anomalies over the North Atlantic (0°–70°N, 80°W–0°) in a winter. The anomaly at each grid point during 1950–2015 was calculated as the deviation from its long-term (1950–2015) mean for each day of the winter.

The method used to identify individual atmospheric blocking events with 10–20 d timescales occurring in the Ural Mountains during 1950–2015 is based on the one-dimensional blocking index of Tibaldi and Molteni (1990) or TM index in terms of meridional gradients of 500 hPa geopotential height. A UB event is defined if the TM index is satisfied in the region (30°–90°E) and persists for at least three consecutive days. We also use a regression-based method to estimate the contributions of the AMO and UB events to the SAT variations in the BKS and central Asia. Mathematically, the linear regression model can be written in the form of $T_A = \alpha\Delta\Sigma + \beta$, where α and β are the regression coefficients, respectively. If the AMO index or UB days is denoted by $\Delta\Sigma$, then T_A represents the AMO- (UB-) related SAT variation.

To reflect the contribution of UB events to the DJF-mean SAT anomaly, we can express the DJF-mean SAT in BKS (central Asia) and 500 hPa zonal wind anomaly fields as $T_{BKS} = \Delta T_{BKS} + \Delta\tilde{T}_{BKS}$($T_C = \Delta T_C + \Delta\tilde{T}_C$) and $U_E = \Delta U_E + \Delta\tilde{U}_E$, where T_{BKS} and T_C are the DJF-mean SAT anomalies in BKS and central Eurasia, respectively; and U_E is the DJF-mean 500 hPa zonal wind anomaly over mid-high latitude Eurasia. Moreover, ΔT_{BKS} (ΔT_C) and ΔU_E represent the DJF-mean SAT and 500 hPa zonal wind anomalies without the UB days respectively. Here, the UB days are defined to be the occurrence days of the UB identified by the TM index. Moreover, $\Delta\tilde{T}_{BKS}$($\Delta\tilde{T}_C$) and $\Delta\ \tilde{U}_E$ denote the DJF-mean values of the SAT and 500 hPa zonal wind anomalies with the UB days, and thus ΔT_{BKS} (ΔT_C) and ΔU_E can be considered as the background or prior conditions of UB events because they do not include the effect of UB events.

3. Results

To understand the possible role of the AMO in the Eurasian air temperature change, it is useful to show the normalized time series of the winter-mean AMO index, SST and SIC anomalies averaged in the BKS in figure 1(*a*). Correspondingly, the normalized time series of the domain-averaged SAT anomalies in the BKS and central Asia (CA: 40°–60°N, 60°–120°E) are shown in figure 1(*b*). It is seen that the winter SAT averaged over central Asia (T_C) has cooled significantly since the early 1990s (Cohen *et al* 2014, McCusker *et al* 2016)

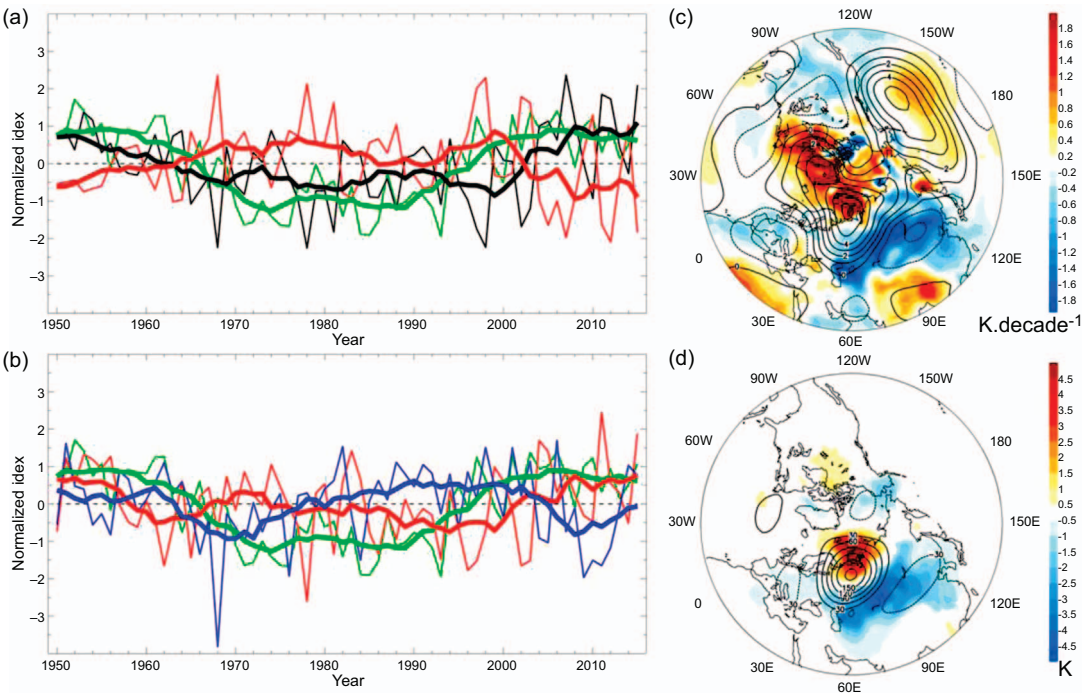

Figure 1. Normalized time series of detrended DJF-mean (*a*) SIC (red line) and SST (black) anomalies averaged over the BKS (65°–85°N, 30°–90°E) and AMO index (green line) and (*b*) SAT anomalies in the BKS (T_{BKS}, red line) and central Asia (40°–60°N, 60°–120°E) (T_C, blue line) during 1950–2015. The thick line denotes a 9 year running average. (*c*) The 1993–2013 trend of DJF-mean SAT (colors, K/decade) and 500 hPa geopotential height (contour: 1 gpm), in which the dots represent the region above the 90% confidence level. (*d*) Composite map of daily SAT (colors, K) and 500 hPa geopotential height (unit: gpm) anomalies averaged from lag −5 to 5 d for UB events during 1950–2015 with lag 0 denoting the peak of the UB. The color shading and contour regions above the 90% confidence level are plotted in panels (*c*)–(*d*). In (*a*)–(*b*), the correlation coefficients for the smoothed curves are *r*(SST, T_{BKS}) = 0.81 *r*(SST, AMO) = 0.70, *r*(SIC, AMO) = −0.63, *r*(T_{BKS}, T_C) = −0.50, and *r* (T_C, AMO) = 0.03.

and this cooling is associated with increasing SAT and SST and decreasing SIC in the BKS, as well as the recent phase change of the AMO (figure 1(*a*) and (*b*)). A decadal cooling from 1960–1973 was also seen over CA when the AMO was on a declining phase, similar to that happened from about 1999–2009 although the AMO index decreased less during this later period (figure 1(*a*) and (*b*)). The detrended DJF-mean SAT in the BKS region (T_{BKS}) exhibits a significant correlation of 0.76 (−0.72) with the SST (SIC) there during 1950–2015. It is also not surprising that the detrended DJF SST and SIC are strongly anti-correlated ($r = -0.95$) in the BKS. The positive SST anomaly in the BKS has been partly attributed to the intrusion of warm Atlantic water into the BKS during AMO positive phases (Levitus *et al* 2009). Luo *et al* (2016b) also found that the SST in the North Atlantic basin is warmer during 2000–2013 than during 1979–1999, which corresponds to a case that the AMO index tends to be positive. We further see that the SAT in BKS has a maximum positive correlation with the AMO index as the later leads the former by about 14 years (figure S1(*a*) available at stacks.iop.org/ERL/12/125002/mmedia). The fact that the detrended SST and SAT (SIC) anomalies on interannual timescales have peak positive (negative) correlations with the AMO index when the later leads the former by about 3 years (figure S1(*a*)) suggests that this intrusion through advection from the northern North Atlantic Ocean into the BKS may take about 3 years. In fact, some studies indicated that the advection time of the Atlantic SST anomaly from the Norwegian Sea to the BSK is of about 2∼3 years (Vinje 2001, Årthun *et al* 2012 Årthun and Eldevik 2016), while the warm Atlantic water has a decadal timescale with a dominant period of 14 years (Eldevik *et al* 2009). To understand the relationship between the SIC, SST and SAT anomalies and the AMO index on a timescale longer than 10 years, their lead-lag correlations are calculated and shown in figure S1(*b*) using a 9 year smoothing. It is obvious that for 9 year smoothed time series, the AMO leads the SIC (SST) in BKS by about 10 (10−12) years and the SAT in BKS by about 10∼16 years (figure S1(*b*)). While we cannot infer the cause and effect relationship between the SST in the BKS and AMO from their correlation coefficient (figure 1(*a*)), it is believed that the high SST over the BKS is partly due to the inflow or advection of the warm Atlantic water into the BKS during the positive AMO (AMO^+) phase (Levitus *et al* 2009, Eldevik *et al* 2009, Årthun *et al* 2012, Årthun and Eldevik 2016) although sea ice loss can enhance the local warming. This notion is consistent with the fact that AMO leads the BKS SST by about 10−12 years (figure S1(*b*)), since the oceanic advection takes a number of years. Gulev *et al* (2013) recently found that on decadal or multidecadal timescales the oceanic process plays a major role in the

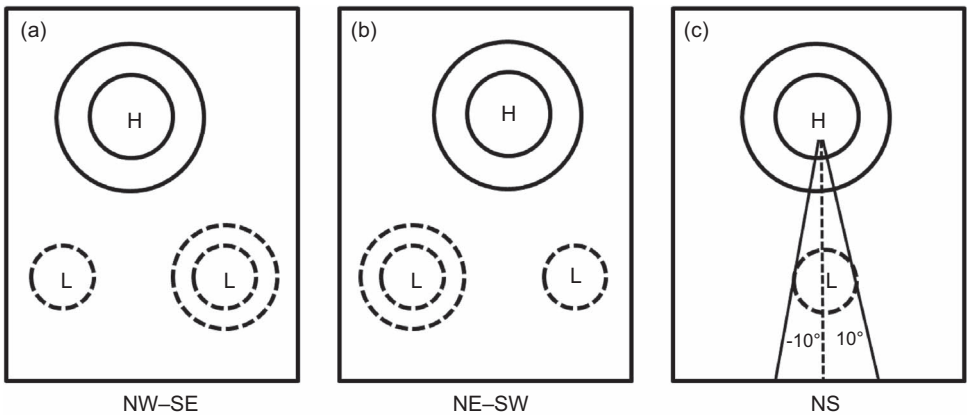

Figure 2. Idealized schematic diagrams of the (*a*) northwest–southeast (NW–SE)-, (*b*) northeast–southwest (NE–SW)- and (*c*) north–south (NS)-oriented UB patterns. The UB is defined as a NW–SE-(NE–SW)-oriented dipole pattern as shown in figures 2(*a*) and (*b*) if the cyclonic anomaly is stronger in the southeast (southwest) side of the anticyclone than in the southwest (southeast) side. The other may be defined as a NS-oriented dipole type, with the center of the cyclonic anomaly located to south of the anticyclone within a range of 20° longitude in figure 2(*c*).

SST change and associated atmospheric variability over the North Atlantic. Thus, an AMO^+ would enhance surface warming over the BKS through the intrusion of warm surface waters from the North Atlantic and the subsequent positive feedback from sea-ice loss (figure S2). This process can amplify the AMO's impact and generate a strong negative correlation ($r = -0.72$) between BKS SIC and T_{BKS} (figure S2(*d*)).

The SAT over CA (T_C) and AMO index show peak correlations when the AMO leads T_C by about 15 (13) years for the unsmoothed (9 year averaged) time series (figure S1(*c*)), although they have no in-phase correlation ($r = 0.03$). This suggests that the AMO could be a cause of the T_C variations. Here we explore the physical links behind this possible cause. As explained above and in other studies, the positive AMO is likely a cause of the recent BKS warming (Chylek *et al* 2009) and sea-ice loss (Day *et al* 2012, Miles *et al* 2014). In fact, the SAT over the BKS and CA is modulated by not only the AMO (Chylek *et al* 2009, Wyatt *et al* 2012), but also by mid-latitude large-scale atmospheric circulations over the Eurasian continent (Luo *et al* 2016a) and North Atlantic (Luo *et al* 2016b). But, how the AMO modulates the Eurasian SAT via the sea-ice loss over the BKS is still unclear, because the linkage between the BKS sea-ice loss and Eurasian cooling is not better established and still controversial (Cohen *et al* 2014, Mori *et al* 2014, Kug *et al* 2015, Outten and Esau 2012, McCusker *et al* 2016). Below we reveal that the AMO-driven BKS warming can cause large Eurasian cooling by changing the frequency, shape and persistence of atmospheric blocking over the Ural Mountains (around 60°E).

One way for the AMO-driven warming over BKS to affect SAT in central Asia is through reducing meridional temperature gradients, which in turn would weaken westerly winds and alter atmospheric circulation over Eurasia (Yao *et al* 2017). Most of Eurasia has undergone pronounced cooling since the early 1990s (Cohen *et al* 2014), and this cooling is associated with a positive height trend in the Ural region (figure 1(*c*)) that resembles the recent change pattern of the UB (Luo *et al* 2016a). The composite SAT and height anomaly patterns associated with UB events (figure 1(*d*)) also match those of the recent SAT and height trend patterns over Eurasia (figure 1(*c*)). These results suggest a possible role of UB in recent Eurasian cooling.

To examine the further impact of UB, we classified the UB events into three types of orientation (figure 2): northwest–southeast (NW–SE)- (figure 2(*a*)), northeast–southwest (NE–SW)- (figure 2(*b*)) and north–south (NS)-oriented (figure 2(*c*)) blocking patterns, similar to Luo *et al* (2015). The total number of the detrended UB events (figure 3(*a*)) is correlated with detrended T_{BKS} (T_C) with a correlation coefficient of 0.35 (−0.41) during 1950–2015 that is statistically significant. It reflects the contribution of UB to the BKS warming and Eurasian cooling (Luo *et al* 2016a). The total number of UB events (figure 3(*a*)) has a peak positive correlation with the AMO index as the AMO leads the UB by about 14 years (figure S3(*a*)). This result is also held for the NW–SE-oriented UB events (red line in figure S3(*b*)). The NS-oriented UB exhibits peak positive correlations with the AMO index as the AMO leads the NS-oriented UB by about 21 years (green line in figure S3(*b*)), while the NE–SW-oriented UB has a peak 6 year leading negative correlation with the AMO (blue line in figure S3(*b*)). For a 9 year moving average the NW–SE- (NS-) oriented UB lags the AMO by about 11 (20) years (figure S3(*c*)). Thus, on decadal or multidecadal timescales the shape and frequency of UB events are related to the phase of the AMO. To examine the impact of the AMO phase on the blocking frequency, during the AMO^+ (1951−59 and 1999−2015) and AMO^- (1968−1992) periods based on ±0.8 standard deviations of the AMO index (figure 1(*a*)) the number of the total UB events and the corresponding ratios of the three blocking types relative to the total UB events can be calculated and shown in figure 3(*f*). We

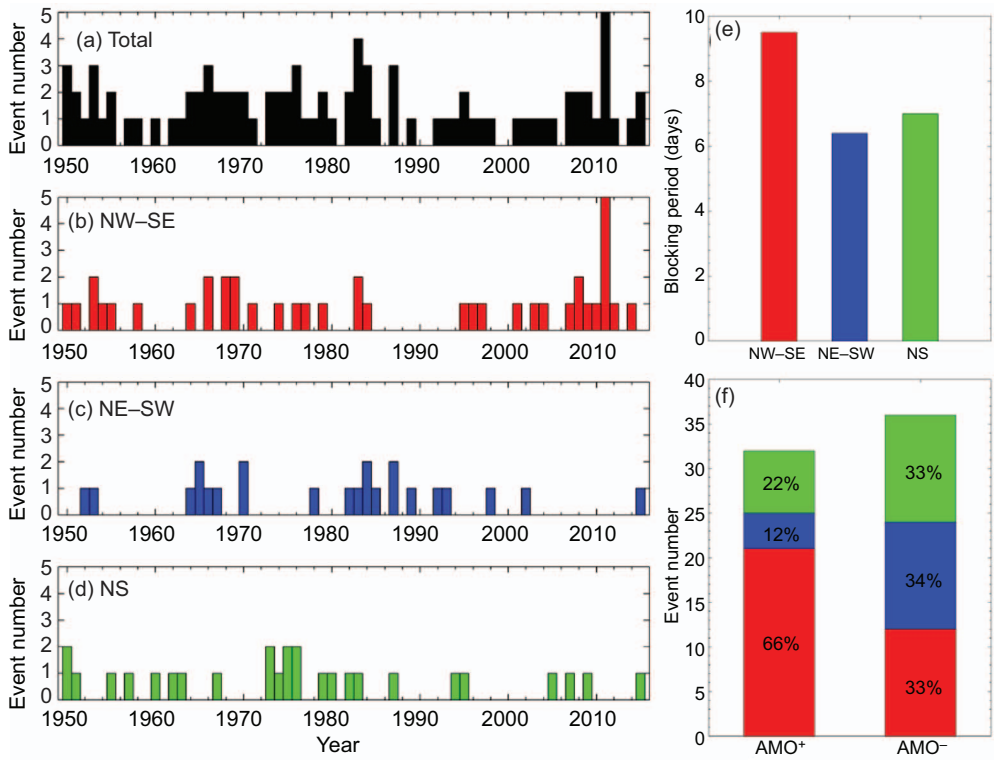

Figure 3. (*a*)–(*d*) Time series of the number of (*a*) total events, (*b*) northwest–southeast- (NW–SE-), (*c*) northeast–southwest- (NE–SW-), and (*d*) north–south- (NS-) oriented UB events during 1950–2015; (*e*) mean blocking durations of NW–SE- (red column), NE–SW-(blue column) and NS- (green column) oriented UB events and (*f*) percentages of NW–SE- (red column), NE–SW- (blue column) and NS- (green column) oriented UB events with respect to the total UB events during the AMO^+ and AMO^- phases during 1950–2015.

see that there are 21 NW–SE- and 4 NE–SW-oriented UB events during the AMO^+ phase, but there are 12 NW–SE- and 12 NE–SW-oriented UB events during the AMO^- phase. While the change of the total UB events from the AMO^- to AMO^+ phases is not significant because it corresponds to a small change from 36 to 32 cases (figure 3(*f*)), the variation of the NW–SE-oriented UB events between the AMO^- and AMO^+ phases is significant. A further calculation shows that the mean duration of the NW–SE-(NE–SW-) oriented UB events is 9.5 (6.4) days, though the NS-oriented UB events have a mean duration of 7 d (figure 3(*e*)). Thus, while the BKS sea-ice loss associated with the AMO^+ phase does not significantly increase the frequency of total UB events, it can correspond to an increased frequency of NW–SE-oriented UB events and the lengthening of their mean life period due to intensified BKS warming. As we show below, the NW–SE-oriented UB pattern associated with AMO^+ can produce a strong winter Eurasian cooling.

The time-mean fields of composite daily geopotential height and SAT anomalies, averaged over a mature period of the UB from lag −5 to 5 day (lag 0 denotes the peak day of the UB), show that the anticyclonic (cyclonic) anomaly of the NW–SE-oriented UB events is stronger (figure 4(*a*)) than the other two types (figures 4(*b*) and (*c*)). The corresponding cold anomaly is also more intense, widespread (blue shading in figure 4(*a*)) and persistent (red line in figure 4(*e*)) than those of NE–SW- and NS-oriented UB events. This is easily explained because the NW–SE-oriented UB is more long-lived than the other two types (figure 3(*e*)) and because the persistent and strong cooling occurs easily over central–eastern Asia through cold advection and radiative cooling (Yao *et al* 2017). While the magnitude of the maximum warming in the BKS is almost the same for NW–SE-, NE–SW- and NS-oriented UB events (figure 4(*d*) for day 0), it seems that the intraseasonal BKS warming of NW–SE-oriented UB events is most persistent amongst the three blocking types (figure 4(*d*)). Thus, the presence of NW–SE-oriented UB events is able to generate a strong, persistent and widespread Eurasian cooling (figure 4(*a*)) and to further amplify the BKS warming prior to the block onset (blue line in figure 4(*d*)).

Here, a key question we need to answer is why the BKS warming is favorable for NW–SE-oriented UB events. The regressed DJF-mean 500 hPa zonal wind against the T_{BKS} time series shows that the Eurasian westerly wind is weakened in mid-high latitudes, but intensified in lower latitudes (figure 4(*f*)). Such a zonal wind distribution will lead to a NW–SE orientation of the UB dipole because the anticyclonic (cyclonic) anomaly of the UB dipole in the reduced (intensified) westerly wind region is displaced westward (eastward). Thus, the BKS ice loss inevitably brings such an effect because the sea ice loss in the BKS corresponds to an intensified warming (figure S2(*d*)), while the BKS

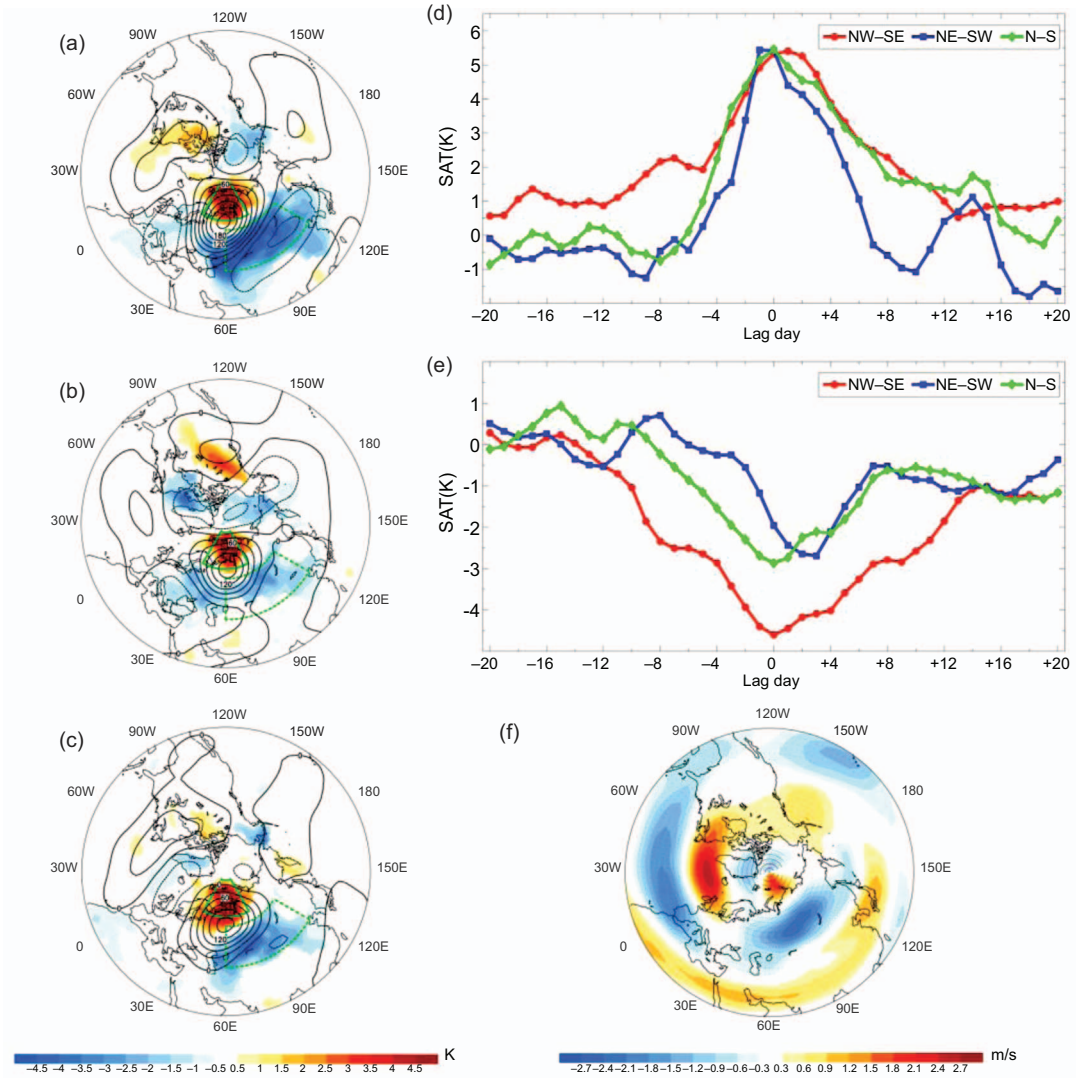

Figure 4. (*a*)–(*c*) Time-mean fields of composite daily 500 hPa geopotential height and SAT anomalies averaged from lag −5 to lag 5 d for NW–SE- (*a*), NE–SW- (*b*) and N-S-oriented (*c*) UB events during 1950–2015, where the solid (dashed) green box denotes the BKS (central Asia); (*d*) and (*e*) time series of composite daily SAT anomalies averaged over the BKS (60°–85°N, 30°–90°E; solid green box) and central Asia (40°–60°N, 60–120°E; dashed green box) for NW–SE- (red line), NE–SW- (blue line) and NS-oriented (green line) UB events and (*f*) regressed field of DJF-mean 500 hPa zonal wind anomaly against the DJF-mean SAT (T_{BKS}) time series over the BKS in figure 1(*b*) (red line). Lag 0 denotes the peak day of the UB. In (*a*)–(*c*), the contour and shading represents the regions above the 95% confidence level, whereas in (*f*) the dot represents the region above the 95% confidence level.

warming includes the effect of the UB. This result is also held for the prior BKS warming without UB days because the prior BKS warming ΔT_{BKS} is highly proportional to the BKS warming (T_{BKS}) with UB days (figure S4(*a*)). The calculation seems to indicate that the Eurasian SAT (ΔT_C) without UB days is unrelated to the prior BKS warming (ΔT_{BKS}) (figure S4(*b*)). This suggests that on an interannual timescale the Eurasian cooling is not directly linked to the BKS warming as the UB is absent, though the Eurasian mid-high latitude westerly wind (EWW) is closely related to the BKS warming (figures S4(*c*) and (*d*)). The DJF-mean warming in the BKS tends to weaken the EWW even for the case without UB days (figure S4(*b*)) through reducing the meridional temperature gradient (not shown). Because the reduced EWW corresponds to an increased persistence of UB (Luo *et al* 2016a, Yao *et al* 2017), the BKS warming lengthens the lifetime of the UB events or increases the blocking days (figures S4(*e*) and (*f*)). Thus, the above results clearly indicate that the BKS ice loss provides an environment that promotes NW–SE-oriented UB events and lengthens their lifetime due to the reduction of the EWW related to BKS warming.

On interannual timescale the BKS warming and Eurasian cooling have no in-phase correlations with the AMO (figures 5(*a*) and (*b*)). However, on a decadal timescale the BKS warming and Eurasian cooling show maximum correlations with the AMO as they lag the later by about 14 years (figure S1). Thus, the AMO may have a delay effect on the Eurasian cooling through the BKS warming. It is expected that the winter Eurasian cooling is strongly modulated by the AMO because the BKS warming corresponds to more UB days (figure 5(*c*)) and because the persistent UB pattern

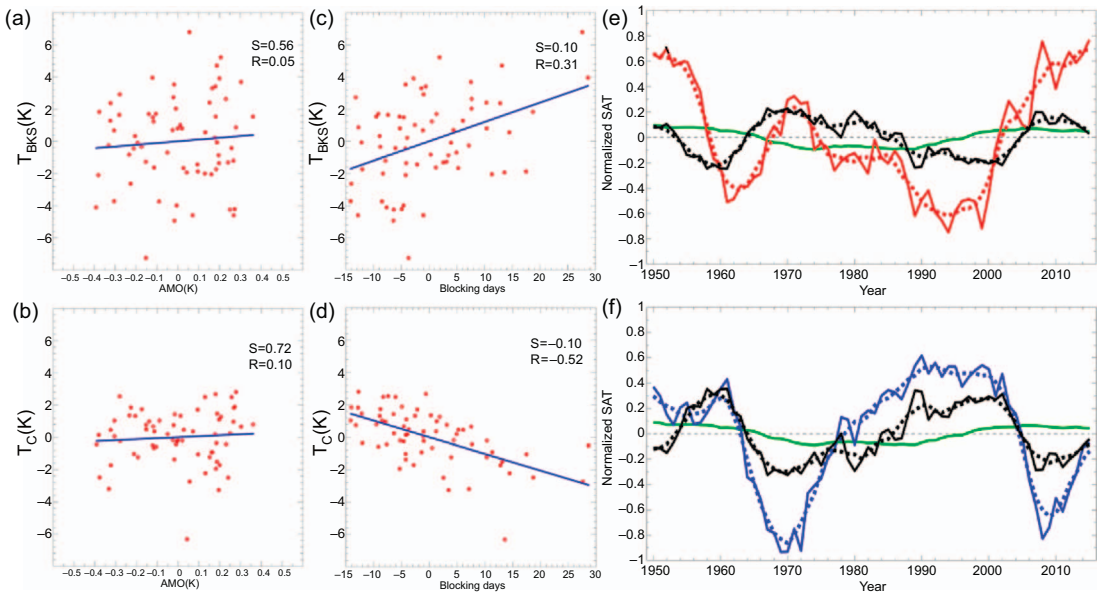

Figure 5. (*a*)–(*d*) Scatter diagram of detrended DJF-mean SAT anomalies (T_{BKS}, T_C) averaged over the BKS (65°–85°N, 30°–90°E) and central Asia (40°–60°N, 60°–120°E) against the detrended AMO index (*a*), (*b*) and blocking days (*c*), (*d*); and (*e*), (*f*) 9 year running average time series of T_{BKS} (*e*) and T_C (f) during 1950–2015. In (*a*)–(*d*), the blue line is the least squares linear best fit. The value of R in the map denotes the correlation coefficient. In (*a*) and (*b*), the slope between T_{BKS} (T_C) and the AMO index is not statistically significant, but in (*c*) and (*d*) the slope between T_{BKS} (T_C) and blocking days is statistically significant at the 95% confidence level. In (*e*)–(*f*), the blue line represents the SAT variation obtained from the reanalysis data and the green (black) line denotes the time series of the regressed AMO- (UB-) driven SAT anomalies over the BKS and Eurasia. The dashed line represents a second 9 year running average. The unit of S is K day^{-1} in (*c*) and (*d*).

leads to a stronger Eurasian cooling (figure 5(*d*)) through cold advection and radiative cooling (Yao *et al* 2017). Thus, it is concluded that the AMO has an important contribution to the Eurasian cooling in winter through the BKS warming and its influence on the UB.

Figures 5(*e*) and (*f*) show the time variations of the SAT anomalies in the BKS and Eurasian continent obtained from reanalysis data (simply defined as an observed one) and the AMO- and UB-induced components using a simple linear regression model. It is found that the AMO-induced SAT anomalies have consistent variations over the BKS and CA regions (green line in figures 5(*e*) and (*f*), though their values are small, thus indicating that the AMO^+ cannot directly produce a cooling in the CA during 2000–2015 if the UB is absent (green line in figure 5(*f*)). The correlation calculation shows that the lagged correlation coefficient of the AMO-induced SAT in BKS with the AMO index is the same as that in CA (figure S5(*a*)). It is also found that the UB-induced BKS SAT variation (black line in figure 5(*e*)) has a significant positive correlation of 0.43 (0.5) with observed T_{BKS} on an interannual timescale (a 9 year moving average). This means that the UB can amplify the AMO-induced BKS warming, although the AMO-induced BKS SAT change is relatively small. Thus, on a decadal timescale the AMO^+ and UB also contribute to the BKS warming. On interannual and decadal (9 year running average) timescales (figure 5(*f*)) in the CA region, while the AMO-induced CA SAT is hardly correlated with observed T_C, the UB-induced CA SAT (black line in figure 5(*f*)) can have a strong positive correlation of 0.59 (0.81) with observed T_C (blue line in figure 5(*f*)). Moreover, it is found that the peak values of the UB-induced BKS warming (figure S5(*b*)) and Eurasian cooling (figure S5(*c*)) lag the AMO by about 14 years. This result is also held for 9 year smoothed time series. Therefrom, it inferred that in the recent decades the UB, especially the NW–SE-oriented UB, has a large contribution to the central Asian cooling through the modulation of the BKS warming triggered by the AMO^+ and enhanced by the sea-ice loss. We further examined the sensitivity of the results in figure 5 to other regression methods such as the Mann–Kendall and robustfit methods. The results were found to be insensitive to the method used (not shown), although based on the reanalysis data. However, it must be pointed out that many other factors such as tropical forcing (Trenberth *et al* 2014), stratospheric processes (Scaife *et al* 2005) and IPO (Dai *et al* 2015) and so on can also influence the winter Eurasian cooling. Thus, how much the AMO contributes to the winter Eurasian cooling compared to these factors needs to be further quantitatively evaluated from different reanalysis and model datasets.

4. Conclusion and discussions

In this paper, we have examined the modulation of the AMO on the winter Eurasian SAT and its contribution to the recent winter Eurasian cooling in the

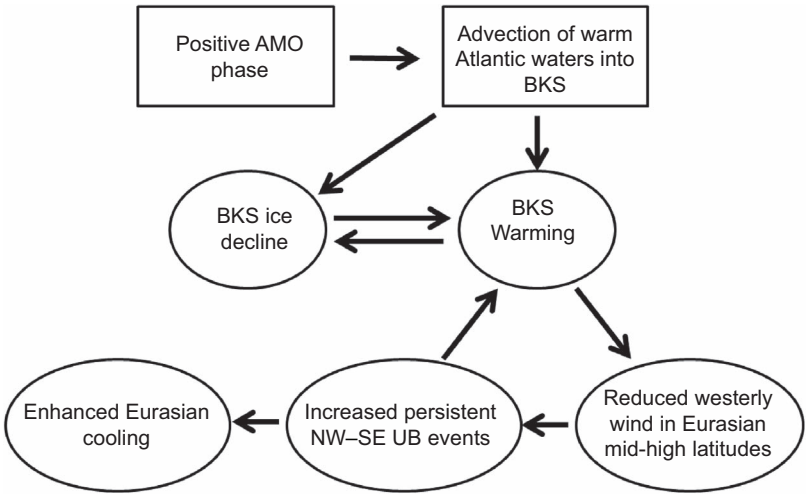

Figure 6. A schematic diagram of the positive AMO phase leading to the winter Eurasian cooling via the increased frequency of NW–SE-oriented UB events due to reduced westerly winds in the Eurasian mid-high latitudes caused by Arctic warming in the Barents–Kara Seas (BKS). The arrow denotes the link direction between two steps and the northwest–southeast is abbreviated as 'NW–SE'.

midlatitudes through analyses of observational and reanalysis data. It is found that the recent positive phase of AMO (AMO^+) causes BKS warming during 1999–2015, likely through the advection of North Atlantic warm surface waters and the positive feedback associated with sea-ice loss. The BKS warming weakens the Eurasian mid-high latitude westerly wind (EWW), which in turn leads to changes in the shape, frequency and persistence of the UB events that contribute to the recent Eurasian cooling. We found that the AMO^+ is able to produce frequent long-lived NW–SE-oriented UB events due to the weakened EWW resulting from the BKS warming. The NW–SE-oriented UB is an optimal circulation pattern that produces a strong, persistent and widespread cold anomaly over Eurasia through cold atmospheric advection and radiative cooling. We also find that the AMO^+ cannot directly generate a cooling over Eurasia if the UB is not present. Thus, the AMO can affect the Eurasian SAT likely only by means of its influence on BKS SST and sea ice, and subsequently the EWW and the frequency, persistence and shape of the UB through the BKS warming. The logic chain of how the AMO^+ leads to the BKS changes and the winter Eurasian cooling since the 1990s is summarized in figure 6 as a schematic diagram. Our results help understand the formation of the recent winter Eurasian cooling (Cohen *et al* 2014, McCusker *et al* 2016) as well as the changes over BKS.

In this paper we did not examine NAO's impact on Eurasian temperatures (Scaife *et al* 2005, Li *et al* 2013), even though the UB is modulated by the phase of the NAO (Luo *et al* 2016b). In fact, the NAO has been found to have an important impact on the Northern Hemisphere air temperature and sea ice near Eurasia (Karpechko *et al* 2015). Eden and Willebrand (2001) indicated that the NAO can drive the North Atlantic SST variability mainly on an interannual to sub-decadal timescale, while Gulev *et al* (2013) found that the surface turbulent heat fluxes driven by the ocean can force the atmosphere on timescales longer than 10 years. To some extent, the AMO may be considered as a driving source for the multi-decadal variability of the SST, SAT and SIC in BKS (Levitus *et al* 2009, Chylek *et al* 2009, Day *et al* 2012, Miles *et al* 2014) and UB. Our results suggest that the winter Eurasian cooling is partly caused by the recent phase change of the AMO due to the AMO-induced decadal or multi-decadal changes in the frequency, persistence and shape of the UB events, in addition to other influences on the Eurasian air temperature such as stratospheric processes (Scaife *et al* 2005). However, further investigations are needed to differentiate the different contributions of the decadal changes in the NAO and UB to the decadal trend of the winter Eurasian cooling, although they are related.

Acknowledgments

The authors acknowledge the support from the National key research and development program of China (2016YFA0601802) and the National Natural Science Foundation of China (Grant numbers: 41430533 and 41375067). The authors would like to thank two anonymous reviewers for their useful suggestions in improving this paper.

ORCID iDs

Dehai Luo https://orcid.org/0000-0001-8834-8623

References

Årthun M, Eldevik T, Smedsrud L H, Ø. S kagseth and Ingvaldsen R B 2012 Quantifying the influence of Atlantic heat on Barents sea ice variability and retreat *J. Clim.* **25** 4736–43

Årthun M T and Eldevik L 2016 On anomalous ocean heat transport toward the Arctic and associated climate predictability *J. Clim.* **29** 689–704
Cohen J *et al* 2014 Recent Arctic amplification and extreme mid-latitude weather *Nat. Geosci.* **7** 627–37
Chylek P *et al* 2009 Arctic air temperature change amplification and the Atlantic multidecadal oscillation *Geophys. Res. Lett.* **36** L14801
Dai A, Fyfe J C, Xie S-P and Dai X 2015 Decadal modulation of global-mean temperature by internal climate variability *Nat. Clim. Change* **5** 555–9
Deser C, Guo R and Lehner F 2017 The relative contributions of tropical Pacific sea surface temperatures and atmospheric internal variability to the recent global warming hiatus *Geophys. Res. Lett.* **44** 7945–54
Day J J, Hargreaves J C, Annan J D and AbeOuchi A 2012 Sources of multidecadal variability in Arctic sea ice extent *Environ. Res. Lett.* **7** 034011
Eden C and Willebrand J 2001 Mechanism of interannual to decadal variability of the North Atlantic circulation *J. Clim.* **14** 2266–80
Eldevik T, Ø Nilsen J E, Iovino D, Olsson K A, Sandø A B and Drange H 2009 Observed sources and variability of nordic seas overflow *Nat. Geosci.* **2** 406–10
Gillett N P *et al* 2008 Attribution of polar warming to human influence *Nat.Geosci.* **1** 750–4
Gulev S K, Latif M, Keenlyside N, Park W and Koltermann K P 2013 North Atlantic ocean control on surface heat flux on multidecadal timescales *Nature* **499** 464–7
Hanna E, Cropper T E, Jones P D, Scaife A A and Allan R 2015 Recent seasonal asymmetric changes in the NAO (a marked summer decline and increased winter variability) and associated changes in the AO and Greenland blocking index *Int. J. Clim.* **35** 2540–54
Hao X, He S and Wang H 2016 Asymmetry in the response of central Eurasian winter temperature to AMO *Clim. Dyn.* **47** 2139–54
Honda M, Inoue J and Yamane S 2009 Influence of low Arctic sea-ice minima on anomalously cold Eurasian winters *Geophys. Res. Lett.* **36** L08707
Huang J P, Xie Y K, Guang X D, Li D D and Ji F 2017 The dynamics of the warming hiatus over the Northern Hemisphere *Clim. Dyn.* **48** 429–46
Knight J R, Allan R J, Folland C K, Vellinga M and Mann M E 2005 A signature of persistent natural thermohaline circulation cycles in observed climate *Geophys. Res. Lett.* **32** L20708
Kug J-S *et al* 2015 Two distinct influences of Arctic warming on cold winters over North America and East Asia *Nat. Geosci.* **8** 759–62
Levitus S, Matishov G, Seidov D and Smolyar I 2009 Barents Sea multidecadal variability *Geophys. Res. Lett.* **36** L19604
Li J, Sun C and Jin F F 2013 NAO implicated as a predictor of Northern Hemisphere mean temperature multidecadal variability *Geophys. Res. Lett.* **40** 5497–502
Luo D, Yao Y, Dai A and Feldstein S 2015 The positive North Atlantic Oscillation with downstream blocking and Middle East snowstorms: the large-scale environment *J. Clim.* **28** 6398–418
Luo D, Xiao Y, Yao Y, Dai A, Simmonds I and Franzke C L E 2016a Impact of ural blocking on winter warm Arctic-cold Eurasian anomalies. Part I: blocking-induced amplification *J. Clim.* **29** 3925–47
Luo D, Xiao Y, Diao Y, Dai A, Franzke C L E and Simmonds I 2016b Impact of Ural blocking on winter warm Arctic-cold Eurasian anomalies. Part II: the link to the North Atlantic oscillation *J. Clim.* **29** 3949–71
Mahajan S, Zhang R and Delworth T L 2011 Impact of the Atlantic meridional overturning circulation (AMOC) on Arctic surface air temperature and sea ice variability *J. Clim.* **24** 6573–81
Mann M E, Park J and Bradley R S 1995 Global interdecadal and century-scale climate oscillations during the past 5 centuries *Nature* **378** 266–70
McCusker K E, Fyfe J C and Sigmond M 2016 Twenty-five winters of unexpected Eurasian cooling unlikely due to Arctic sea-ice loss *Nat. Geosci.* **9** 838–8431
Miles M W *et al* 2014 A signal of persistent Atlantic multidecadal variability in Arctic sea ice *Geophys. Res. Lett.* **41** 463–9
Mori M, Watanabe M, Shiogama H, Inoue J and Kimoto M 2014 Robust Arctic sea-ice influence on the frequent Eurasian cold winters in past decades *Nat. Geosci.* **7** 869–73
Omrani N E, Keenlyside N S, Bader J and Manzini E 2014 Stratosphere key for wintertime atmospheric response to warm Atlantic decadal conditions *Clim. Dyn.* **42** 649–63
Outten S and Esau I 2012 A link between Arctic sea ice and recent cooling trends over Eurasia *Clim. Change* **110** 1069–75
Overland J E *et al* 2016 Nonlinear response of mid-latitude weather to the changing Arctic *Nat. Clim. Change* **6** 992–8
Scaife A A, Knight J R, Vallis G K and Folland C K 2005 A stratospheric influence on the winter NAO and North Atlantic surface climate *Geophys. Res. Lett.* **32** L18715
Semenov V A and Latif M 2015 Nonlinear winter atmospheric circulation response to Arctic sea ice concentration anomalies for different periods during 1966–2012 *Environ. Res. Lett.* **10** 054020
Steinman B A, Mann M E and Miller S K 2015 Atlantic and Pacific multidecadal oscillations and Northern Hemisphere temperatures *Science* **347** 988–90
Tibaldi S and Molteni F 1990 On the operational predictability of blocking *Tellus* **42A** 343–65
Trenberth K E, Fasullo J T, Branstator G and Phillips A S 2014 Seasonal aspects of the recent pause in surface warming *Nat. Clim. Change* **4** 911–6
Vinje T 2001 Anomalies and trends of sea ice and atmospheric circulation in the Nordic Seas during the period 1864–1998 *J. Clim.* **14** 255–67
Wang L, Ting M and Kushner P J 2017 A robust empirical seasonal prediction of winter NAO and surface climate *Sci. Rep.* **7** 279
Wyatt M G S, Kravtsov S and Tsonis A 2012 Atlantic multidecadal oscillation and Northern Hemisphere's climate variability *Clim. Dyn.* **38** 929–49
Yao Y, Luo D, Dai A and Simmonds I 2017 Increased quasi-stationarity and persistence of Ural blocking and Eurasian extreme cold events in response to Arctic warming. Part I: Insight from observational analyses. *J. Clim.* **30** 3549–68
Yu Karpechko A, Peterson K A, Scaife A A, Vainio J and Gregow H 2015 Skilful seasonal predictions of Baltic sea ice cover *Environ. Res. Lett.* **10** 044007